Mesenchymal stem cells attenuate peripheral neuronal degeneration in spinocerebellar ataxia type 1 knockin mice

Tokue Mieda[1], Nana Suto[2], Akira Iizuka[2], Serina Matsuura[2], Haku Iizuka[1], Kenji Takagishi[1], Kazuhiro Nakamura[2] and Hirokazu Hirai[2,*]

Department of [1]Orthopedic Surgery and [2]Neurophysiology & Neural Repair, Gunma University Graduate School of Medicine, 3-39-22, Showa-machi, Maebashi, Gunma, 371-8511 Japan

[*]To whom correspondence should be addressed.

Hirokazu Hirai, Phone: 81-27-220-7930, Fax: 81-27-220-7936

E-mail: hirai@ gunma-u.ac.jp

Keywords: MSC, SCA1, spinal motor neuron, myelin, axon

Abbreviations: ADL, Activity of Daily Living Scale; ANOVA, analyses of variance; ATXN-1, ataxin-1; BBS, Berg Balance Scale; CNS, central nervous system; ICARS, Cooperative Ataxia Rating Scale; MBP, myelin basic protein; MSCs, mesenchymal stem cells; PCs, Purkinje cells; PNS, peripheral nervous system; SCA1, spinocerebellar ataxia type 1; Tg, transgenic; UCMSCs, umbilical cord MSCs; WT, wild-type.

Abstract

Spinocerebellar ataxia type 1 (SCA1) is a devastating neurodegenerative disorder in which an abnormally expanded polyglutamine tract is inserted into causative ataxin-1 proteins. We have previously shown that SCA1-knockin (SCA1-KI) mice over 6 months of age exhibit a degeneration of motor neuron axons and their encasing myelin sheaths, as reported in SCA1 patients. Here, we studied whether axon degeneration precedes myelin degeneration, or vice versa, in SCA1-KI mice. We then attempted to mitigate motor neuron degeneration by intrathecally administering MSCs. Temporal examination of the diameters of motor neuron axons and their myelin sheaths revealed a decrease in diameter of the axon, but not of the myelin sheaths, in SCA1-KI mice as early as 1 month of age, which suggests the secondary degeneration of the myelin sheaths. We injected MSCs into the intrathecal space of SCA1-KI mice at 1 month of age, which resulted in a significant suppression of degeneration of both motor neuron axons and myelin sheaths, even 6 months following the MSC injection. Thus, MSCs effectively suppressed peripheral nervous system degeneration in SCA1-KI mice. It has not yet been clarified how clinically administered MSCs exhibit significant therapeutic effects in patients with SCA1. The morphological evidence presented in this current mouse study might explain the mechanisms that underlie the therapeutic effects of MSCs that are observed in patients with SCA1.

Significance statement

Currently, there are no effective treatments for patients with SCA1. We have previously shown that SCA1-knockin (SCA1-KI) mice exhibit a degeneration of motor neuron axons and myelin sheaths in the spinal cord, as reported in patients with SCA1. In the current study, we challenged motor neuron degeneration by intrathecally administering mesenchymal stem cells (MSCs). A single intrathecal injection of MSCs into non-symptomatic SCA1-KI mice at 1 month of age ameliorated the progressive degeneration of both axons and myelin in the spinal cord, even 6 months following the MSC injection. These results suggest the utility of MSCs in the treatment of the peripheral neuronal pathology that is observed in patients with SCA1.

Introduction

Ataxia is caused by the degeneration of neurons in various brain regions, including the brainstem, cerebellum, and spinocerebellar tracts, as well as their afferent and efferent connections (reviewed in (Orr 2012)). Among over 50 different types of inherited ataxias (Manto 2005; Taroni and DiDonato 2004), spinocerebellar ataxia type 1 (SCA1) is caused by the ataxin-1 protein (ATXN1) that contains an abnormally expanded polyglutamine (Matilla-Duenas et al. 2008). SCA1 is characterized by the neurodegeneration of a broad range of the central nervous system (CNS) (Robitaille et al. 1995), including the cerebral cortex, basal ganglia, brainstem and cerebellum. The signs and symptoms of SCA1 include cerebellar ataxia and other neurological signs, such as pyramidal signs, ophthalmoplegia and cognitive impairment (Harding 1983).

Mesenchymal stem cells (MSCs) are present in the umbilical cord blood, bone marrow and adipose tissue (Baddoo et al. 2003; Gimble and Guilak 2003; Lee et al. 2004) and function as multipotent progenitor cells. MSCs can differentiate into mesenchymal lineage cells, such as osteoblasts, adipocytes and chondrocytes, and into other cell lineages, such as glial cells and hepatocytes (Lagasse et al. 2000; Pittenger et al. 1999; Woodbury et al. 2002). In addition to the direct differentiation of MSCs, trophic factors that are released from MSCs may act on neurons through bone marrow-derived hepatocyte growth factor (HGF), fibroblast growth factor-2 (FGF-2), insulin-like growth factor-1 (IGF-1) and vascular endothelial growth factor (VEGF). These factors have been previously detected in MSC-conditioned medium (Olson et al. 2012). Their potential clinical applications in the treatment of neurodegenerative disorders (Mazzini et al. 2010) and stroke (Chen et al. 2003; Li et al. 2005) have also been studied.

We previously demonstrated that intrathecally injected KUM10 cells, which is a bone

marrow-derived MSC cell line, markedly ameliorated the degeneration of cerebellar neurons (Matsuura et al. 2014), particularly cerebellar Purkinje cells (PCs), in SCA1-transgenic (SCA1-Tg) mice that expressed an ATXN1 sequence with an 82 CAG repeat expansion (Burright et al. 1995; Clark et al. 1997). The cerebella of the untreated SCA1-Tg mice developed ectopically located PC somata that formed a multi-PC layer alignment and a thinner molecular layer. Following the intrathecal injection of MSCs, the treated SCA1-Tg mice exhibited a single layer of PCs and a thicker molecular layer (Matsuura et al. 2014). In addition, the SCA1-Tg mice exhibited a significant preservation of the PC dendrites following MSC treatment. The MSC-treated mice also improved their motor coordination performance to a level that was nearly indistinguishable from the wild type (WT) mice (Matsuura et al. 2014).

Patients with SCA1 also exhibit degeneration of the peripheral nervous system (PNS). Eleven autopsied cases of SCA1-type olivopontocerebellar atrophy displayed a neuronal cell loss of the motor neurons in both the lumbo-sacral cord and the thin anterior spinal roots (Robitaille et al. 1995). Similarly, Klüver-Barrera staining of the cervical spinal cord from a patient with SCA1-type olivopontocerebellar atrophy demonstrated a marked loss of myelin in multiple areas (Robitaille et al. 1995).

Given the mitigation of CNS pathology in SCA1-Tg mice, we were motivated to determine the effect of MSCs on their PNS pathology. The SCA1-knockin (SCA1-KI) mouse (Watase et al. 2002) is a suitable experimental animal because it reliably replicates the PNS pathology that is observed in patients with SCA1. For example, some spinal motor neurons of the SCA1-KI mice at 6 months of age have polyglutamine aggregates in their nuclei as well as thinner axons whose myelin sheaths are of irregular sizes in the ventral root (Takechi et al. 2013). This indicates that both spinal motor

neurons and the myelin that covers their axons are degenerated in old SCA1-KI mice. Theoretically, primary demyelination could result in secondary axonal injury (the outside-in model); in turn, primary axonopathy might induce secondary demyelination (the inside-out model) (Tsunoda and Fujinami 2002). It has not yet been determined which structure experiences degeneration earlier in SCA1-KI mice. In this investigation, axon degeneration, but not myelin degeneration, was shown to occur as early as 1 month of age in SCA1-KI mice. Furthermore, it was shown that the intrathecal injection of MSCs during the non-symptomatic stage (1 month old) mitigated the subsequent degeneration of both neurons and myelin in the PNS.

Materials and Methods

Mice

WT and SCA1-KI C57BL/6 mice (kindly provided by Dr. Mizusawa at Tokyo Medical and Dental University) were used for all experiments. Animal care and treatments were performed according to the NIH guidelines and were approved by the Animal Resource Committees of Gunma University. All efforts were made to minimize suffering and to reduce the number of animals that were used in the experiments. Some mice received intrathecal injections of MSCs at 5 weeks of age.

Histology

Mice were transcardially perfused with 4% paraformaldehyde in a solution of 0.1 M phosphate buffer, pH 7.4. The entire vertebra and the enclosed spinal cord were post-fixed in the same fixative solution overnight at 4°C. After decalcification, a transverse lumbar vertebral block that was 2 mm in thickness (L5) was dissected.

Sections of 5 μm in thickness were prepared from paraffin blocks using a microtome. After deparaffinization and treatment with graded alcohol, the sections were processed for HE staining or immunofluorescence staining with anti-β-tubulin (Sigma, St. Louis, MO, T4026, AB_477577), anti-myelin basic protein (MBP) (Santa Cruz Biotechnology, CA, SC-13914, AB_648798) and/or anti-GFP antibodies. Immunofluorescence staining was performed as previously described (Nakamura et al. 2012). Briefly, the sections were incubated with primary antibodies overnight at 4°C. The sections were subsequently treated with Alexa Fluor 488- and Cy3-conjugated secondary antibodies (Jackson ImmunoResearch, West Grove, PA). The fluorescent signals were observed using a confocal microscope (LSM5, Carl Zeiss, Oberkochen, Germany).

To quantify the size of the axons, the diameter of the short axis of the transverse myelinated axons was measured from the β-tubulin staining images. For myelin quantification, the diameter of the short axis of the myelin inner circle was measured from the MBP staining images. We measured the diameters of axons and myelin using Image J software.

Culture of MSCs

KUM10, a mesenchymal stem cell line that was generated from C57/BL6 mouse bone marrow, was purchased from the RIKEN BioResource Center. The cells were cultured in M061101 medium that contained 10% FBS and antibiotics (GP BioSciences, Yokohama, Japan) and were maintained in 5% CO_2 at 37°C unless otherwise specified.

Verification of MSC penetration into the spinal cord

SCA1-KI mice were heavily anesthetized with ketamine hydrochloride (100 mg/kg) and

xylazine hydrochloride (10 mg/kg) before being placed in a stereotaxic apparatus. GFP-labeled MSCs were suspended in 10 μl of DMEM that contained 15% FBS, 2 mM L-glutamine, 1 mM pyruvic acid, non-essential amino acid, 2-mercaptoethanol and antibiotics and were then injected into the subarachnoid space at the level of the lumber spinal cord using a syringe.

We first verified that the MSCs were properly loaded in the subarachnoid space by HE staining and immunostaining of the spinal cord sections immediately following the injection of MSCs (1 x 10^6 cells). Then, 1 h or 3 days after MSC administration (1.5 x 10^5 cells), paraffin sections of the spinal cord were prepared, and the presence of GFP-labeled MSCs was examined.

Intrathecal injection of MSCs

The heavily anesthetized mice were fixed on the stereotaxic apparatus. The suboccipital skin between the occipital bone and the cervical spine was incised and the meninges that covered the medulla oblongata were exposed. A 30-G disposable needle (BD, Franklin Lakes, NJ) was inserted into the subarachnoid space. After the evacuation of approximately 15 μl of cerebrospinal fluid, a suspension of 3 × 10^3 MSCs in 10 μl of the culture medium was injected over the course of 1 min using a Hamilton syringe.

Statistical analysis

The values that were obtained are expressed as the mean ± the S.E.M. Statistical analyses of the differences between the groups were performed with one-way analyses of variance (ANOVAs) followed by a Tukey's post hoc test or Wilcoxon test. P values less than 0.05 were considered statistically significant.

Results

MSCs loaded into the subarachnoid space approach to axons in the root

In our previous study, MSCs were shown to successfully attenuate the cerebellar pathology that was identified in SCA1-Tg mice (Matsuura et al. 2014) in which we demonstrated the entry of intrathecally administered MSCs into the cerebellum. Similarly, we anticipated that intrathecally injected MSCs would localize adjacent to spinal neurons to benefit the spinal neurons of SCA1-KI mice. To examine the localization of intrathecally injected MSCs, we injected GFP-labeled MSCs into the subarachnoid space at the level of the lumber spinal cord and traced them.

We first checked immediately after injection if the MSCs were properly loaded into the subarachnoid space. HE staining of the section revealed the penetration of dura and arachnoid mater by the needle and entry of MSCs into the subarachnoid space through the perforated dura and arachnoid mater (Fig. 1A, B). The cells proved MSCs because the cells have GFP signals (Fig. 1C). One hour after MSC administration, GFP-labeled MSCs were found in the region that was adjacent to MBP-positive myelinated axons in the root (Fig. 1D, E). The same results were observed in the section three days after MSC injection: GFP-labeled MSCs were identified in the region that was close to axons in the ventral root (Fig. 1F, G). The localization of MSCs in the region adjacent to axons potentially enables the transfer of unidentified trophic factors from MSCs to spinal axons. The factors might then be able to act focally in the axons and myelin or might be transported to the soma.

Axonal degeneration precedes myelin degeneration in spinal motor neurons in

young SCA1-KI mice

Previously, we demonstrated the degeneration of both motor neuron axons and myelin sheaths in old SCA1-KI mice (Takechi et al. 2013). Here, we sought to determine which structure initially degenerates and when the degeneration occurs.

At 7 months of age, both the axon and myelin diameters were significantly shorter in the SCA1-KI mice (1.89 ± 0.07 and 2.16 ± 0.07 μm, axon and myelin, respectively) compared with the WT mice (3.62 ± 0.08 and 3.97 ± 0.10 μm, axon and myelin, respectively) (Wilcoxon, $p < 0.001$ each) (Fig. 2A-C). Because 7 months of age allowed for sufficient time to exhibit the degeneration of both axons and myelin, we performed the same quantification using 3-month-old mice. However, the sizes of both the axon and myelin were still significantly smaller in the SCA1-KI mice (2.34 ± 0.08 and 2.49 ± 0.09 μm, axon and myelin, respectively) than in the WT mice (3.40 ± 0.08 and 3.32 ± 0.09 μm, axon and myelin, respectively) (Wilcoxon, $p < 0.001$ each) (Fig. 2D-F). Then, we examined 1-month-old mice. Remarkably, a subtle but significantly smaller axon size was identified in the SCA1-KI mice (1.78 ± 0.04 μm) compared with the WT mice (2.12 ± 0.04 μm) (Wilcoxon, $p < 0.001$), whereas the diameter of the inner circle of myelin was nearly identical between the genotypes (2.34 ± 0.04 and 2.42 ± 0.06 μm, WT and SCA1-KI, respectively) (Wilcoxon, $p = 0.434$) (Fig. 2G-I). These results suggest that the axon degeneration begins as early as 1 month of age, when SCA1-KI mice are still non-symptomatic. Then, the preceding axon degeneration likely causes the secondary degeneration of the myelin sheath between 1 and 3 months of age.

MSCs attenuate the degeneration of both axons and myelin of spinal motor neurons in SCA1-KI mice.

Because earlier treatment may yield more beneficial outcomes, we administered KUM10 MSCs into the SCA1-KI mice at 5 weeks of age when subtle axonal, but not myelin, degeneration was occurring. We applied a single intrathecal injection of 3×10^3 MSCs into the mice and examined whether the MSCs suppressed the progressive degeneration of both spinal motor neuron axons and myelin at 7 months of age.

Double immunolabeling of the ventral root of the lumber spinal cord from the WT, untreated SCA1-KI and MSCs-treated SCA1-KI mice was performed using anti-β-tubulin and anti-MBP antibodies. Again, the untreated SCA1-KI mice exhibited smaller axon and myelin sizes (1.89 ± 0.07 and 2.16 ± 0.07 μm, axon and myelin, respectively) than did the WT mice (3.62 ± 0.08 and 3.97 ± 0.10 μm, axon and myelin, respectively) (ANOVA followed by a Tukey's post hoc test, $p < 0.001$ each) (Fig. 3A-C). In contrast, the MSC-treated SCA1-KI mice exhibited larger axon and myelin sizes (2.89 ± 0.08 and 2.88 ± 0.84 μm, axon and myelin, respectively) compared with the untreated SCA1-KI mice (1.89 ± 0.07 and 2.16 ± 0.07 μm, axon and myelin, respectively) (ANOVA followed by a Tukey's post hoc test, $p < 0.001$ each) (Fig. 3A-C). Thus, MSCs that were administered during the non-symptomatic stage significantly ameliorated the progressive degeneration of both axons and myelin in the peripheral nervous system in SCA1-KI mice.

Discussion

In the present study, we demonstrated that an intrathecal injection of only 3×10^3 MSCs during the non-symptomatic stage mitigated the degeneration of PNS neurons even 6 months following the MSC injection. The decreases in the diameters of motor neuronal axons and the myelin sheaths in SCA1-KI mice were significantly suppressed by MSC

treatment (Fig. 3). In our previous study, the same administration protocol of MSCs attenuated the cerebellar neuronal pathology and consequently resulted in a significantly improved rotarod performance in SCA1-Tg mice (Matsuura et al. 2014). Although it is still preliminary, a similar behavioral improvement following MSC injection was also observed in SCA1-KI mice (data not shown). Thus, MSCs exert therapeutic effects on the pathologies of both CNS and PNS neurons and presumably on the behavior of SCA1-model mice.

We have already reported the degeneration of myelin that covers the motor neuron axons in SCA1-KI mice (Takechi et al. 2013), as observed in patients with SCA1 (Robitaille et al. 1995). Nevertheless, it remains elusive whether the myelin degeneration was a primary event or a lesion secondary to axonal degeneration. To clarify this, we examined the temporal change of the diameters of motor neuron axons and myelin sheaths in SCA1-KI mice. Eventually, we found that the axonal degeneration occurred earlier (i.e., as early as one month old) than did the myelin degeneration, which suggests an inside-out model in which primary axonopathy induces secondary demyelination (Tsunoda and Fujinami 2002). Consistent with this idea, we identified polyglutamine aggregates in some nuclei of spinal motor neurons (Takechi et al. 2013), but not in Schwann cells (data not shown).

To the best of our knowledge, only two studies have reported the efficacy and safety of MSCs in SCA patients. In one study from 2011, umbilical cord-derived MSCs (UCMSCs) were used for SCA patients (Dongmei et al. 2011). The International Cooperative Ataxia Rating Scale (ICARS) and the Activity of Daily Living Scale (ADL) scores reflecting the motor function and quality of daily life were significantly improved 1 month following the use of MSCs in treatment.

In a 2013 study that administered UCMSCs to SCA patients, 16 genomically diagnosed SCA patients, including 5 cases of SCA1, 4 cases of SCA2 and 7 cases of SCA3, received infusions of UCMSCs (Jin et al. 2013). According to the ICARS, the patients experienced an amelioration of neural dysfunction, which was significant at the 3rd and 6th months (Jin et al. 2013). Collectively, it appears that UCMSCs improve the movement ability and quality of daily life for at least several months without inducing serious side effects.

There is no consensus regarding the optimal dose of stem cells or the optimal route of administration during treatment. Our dose of MSCs for mice in the previous (Matsuura et al. 2014) and the current study is approximately 10-100 times lower than the dose used in human studies. Thus, lower doses might be sufficient to obtain therapeutic effects in SCA patients.

The mechanisms by which MSCs relieve the degeneration of neurons in the PNS do not appear to rely on the direct differentiation of MSCs into neurons and/or glia because the number of engrafted MSCs in this study was only 3×10^3. Instead, trophic factors that are released from MSCs may act on neurons as HGF and its primary receptor, cMet, have been found to be critical for bone marrow-derived MSC-mediated recovery in a mouse model of multiple sclerosis, neural cell development and remyelination (Bai et al. 2012). Here, we showed the localization of MSCs in close proximity to the axons in the spinal root, thus suggesting a potential interaction of trophic factors, which are released from MSCs, with the degenerating motor neurons. Reina et al. demonstrated the presence of natural perforations throughout the surface of the lumbar pia mater in humans, which could facilitate the diffusion of substances to the spinal cord following subarachnoid administration (Reina et al. 1998). Given that similar perforations also

exist in the mouse pia mater, they could serve as routes for MSC-derived therapeutic factors to enter the spinal cord. We are currently working on a project to study the therapeutic efficacy of MSC-conditioned media in SCA1-model mice, which will answer the question of whether factors that are released from MSCs underlie the beneficial influence observed in the PNS of SCA1-KI mice.

Conflicts of interest statement

There are no potential conflicts of interest in the content of this paper.

Authors roles

Tokue Mieda, Akira Iizuka, Nana Suto, Serina Matsuura and Kazuhiro Nakamura performed the experiments. Tokue Mieda performed the data analyses. Kazuhiro Nakamura, Kenji Takagishi, Haku Iizuka and Hirokazu Hirai designed the experiments. Kazuhiro Nakamura and Hirokazu Hirai wrote the manuscript.

Acknowledgements

This work was supported by MEXT KAKENHI Grant Number 26111701, grants from the Research on Measures for Intractable Diseases (Ataxic Diseases and Neurodegenerative Diseases) from the Ministry of Health, Labour and Welfare, Gunma University Initiative for Advanced Research (GIAR) (to H. Hirai) and grants-in aid for Scientific Research from the Ministry of Education, Culture, Sports, Science and Technology of Japan (to K. Nakamura).

References

Baddoo M, Hill K, Wilkinson R, Gaupp D, Hughes C, Kopen GC, Phinney DG. 2003. Characterization of mesenchymal stem cells isolated from murine bone marrow by negative selection. Journal of cellular biochemistry 89(6):1235-1249.

Bai L, Lennon DP, Caplan AI, DeChant A, Hecker J, Kranso J, Zaremba A, Miller RH. 2012. Hepatocyte growth factor mediates mesenchymal stem cell-induced recovery in multiple sclerosis models. Nature neuroscience 15(6):862-870.

Burright EN, Clark HB, Servadio A, Matilla T, Feddersen RM, Yunis WS, Duvick LA, Zoghbi HY, Orr HT. 1995. SCA1 transgenic mice: a model for neurodegeneration caused by an expanded CAG trinucleotide repeat. Cell 82(6):937-948.

Chen J, Li Y, Katakowski M, Chen X, Wang L, Lu D, Lu M, Gautam SC, Chopp M. 2003. Intravenous bone marrow stromal cell therapy reduces apoptosis and promotes endogenous cell proliferation after stroke in female rat. Journal of neuroscience research 73(6):778-786.

Clark HB, Burright EN, Yunis WS, Larson S, Wilcox C, Hartman B, Matilla A, Zoghbi HY, Orr HT. 1997. Purkinje cell expression of a mutant allele of SCA1 in transgenic mice leads to disparate effects on motor behaviors, followed by a progressive cerebellar dysfunction and histological alterations. The Journal of neuroscience : the official journal of the Society for Neuroscience 17(19):7385-7395.

Dongmei H, Jing L, Mei X, Ling Z, Hongmin Y, Zhidong W, Li D, Zikuan G, Hengxiang W. 2011. Clinical analysis of the treatment of spinocerebellar ataxia and multiple system atrophy-cerebellar type with umbilical cord mesenchymal stromal cells. Cytotherapy 13(8):913-917.

Gimble J, Guilak F. 2003. Adipose-derived adult stem cells: isolation, characterization, and differentiation potential. Cytotherapy 5(5):362-369.

Harding AE. 1983. Classification of the hereditary ataxias and paraplegias. Lancet 1(8334):1151-1155.

Jin JL, Liu Z, Lu ZJ, Guan DN, Wang C, Chen ZB, Zhang J, Zhang WY, Wu JY, Xu Y. 2013. Safety and efficacy of umbilical cord mesenchymal stem cell therapy in hereditary spinocerebellar ataxia. Current neurovascular research 10(1):11-20.

Lagasse E, Connors H, Al-Dhalimy M, Reitsma M, Dohse M, Osborne L, Wang X, Finegold M, Weissman IL, Grompe M. 2000. Purified hematopoietic stem cells can differentiate into hepatocytes in vivo. Nature medicine 6(11):1229-1234.

Lee OK, Kuo TK, Chen WM, Lee KD, Hsieh SL, Chen TH. 2004. Isolation of multipotent mesenchymal stem cells from umbilical cord blood. Blood

103(5):1669-1675.

Li Y, Chen J, Zhang CL, Wang L, Lu D, Katakowski M, Gao Q, Shen LH, Zhang J, Lu M, Chopp M. 2005. Gliosis and brain remodeling after treatment of stroke in rats with marrow stromal cells. Glia 49(3):407-417.

Manto MU. 2005. The wide spectrum of spinocerebellar ataxias (SCAs). Cerebellum 4(1):2-6.

Matilla-Duenas A, Goold R, Giunti P. 2008. Clinical, genetic, molecular, and pathophysiological insights into spinocerebellar ataxia type 1. Cerebellum 7(2):106-114.

Matsuura S, Shuvaev AN, Iizuka A, Nakamura K, Hirai H. 2014. Mesenchymal stem cells ameliorate cerebellar pathology in a mouse model of spinocerebellar ataxia type 1. Cerebellum 13(3):323-330.

Mazzini L, Ferrero I, Luparello V, Rustichelli D, Gunetti M, Mareschi K, Testa L, Stecco A, Tarletti R, Miglioretti M, Fava E, Nasuelli N, Cisari C, Massara M, Vercelli R, Oggioni GD, Carriero A, Cantello R, Monaco F, Fagioli F. 2010. Mesenchymal stem cell transplantation in amyotrophic lateral sclerosis: A Phase I clinical trial. Experimental neurology 223(1):229-237.

Nakamura K, Kosugi I, Lee DY, Hafner A, Sinclair DA, Ryo A, Lu KP. 2012. Prolyl isomerase Pin1 regulates neuronal differentiation via beta-catenin. Molecular and cellular biology 32(15):2966-2978.

Olson SD, Pollock K, Kambal A, Cary W, Mitchell GM, Tempkin J, Stewart H, McGee J, Bauer G, Kim HS, Tempkin T, Wheelock V, Annett G, Dunbar G, Nolta JA. 2012. Genetically engineered mesenchymal stem cells as a proposed therapeutic for Huntington's disease. Molecular neurobiology 45(1):87-98.

Orr HT. 2012. Cell biology of spinocerebellar ataxia. The Journal of cell biology 197(2):167-177.

Pittenger MF, Mackay AM, Beck SC, Jaiswal RK, Douglas R, Mosca JD, Moorman MA, Simonetti DW, Craig S, Marshak DR. 1999. Multilineage potential of adult human mesenchymal stem cells. Science 284(5411):143-147.

Reina MA, Lopez Garcia A, de Andres JA. 1998. [Anatomical description of a natural perforation present in the human lumbar pia mater]. Revista espanola de anestesiologia y reanimacion 45(1):4-7.

Robitaille Y, Schut L, Kish SJ. 1995. Structural and immunocytochemical features of olivopontocerebellar atrophy caused by the spinocerebellar ataxia type 1 (SCA-1) mutation define a unique phenotype. Acta neuropathologica 90(6):572-581.

Takechi Y, Mieda T, Iizuka A, Toya S, Suto N, Takagishi K, Nakazato Y, Nakamura K, Hirai H. 2013. Impairment of spinal motor neurons in spinocerebellar ataxia type 1-knock-in mice. Neuroscience letters 535:67-72.

Taroni F, DiDonato S. 2004. Pathways to motor incoordination: the inherited ataxias. Nature reviews Neuroscience 5(8):641-655.

Tsunoda I, Fujinami RS. 2002. Inside-Out versus Outside-In models for virus induced demyelination: axonal damage triggering demyelination. Springer Semin Immunopathol 24(2):105-125.

Watase K, Weeber EJ, Xu B, Antalffy B, Yuva-Paylor L, Hashimoto K, Kano M, Atkinson R, Sun Y, Armstrong DL, Sweatt JD, Orr HT, Paylor R, Zoghbi HY. 2002. A long CAG repeat in the mouse Sca1 locus replicates SCA1 features and reveals the impact of protein solubility on selective neurodegeneration. Neuron 34(6):905-919.

Woodbury D, Reynolds K, Black IB. 2002. Adult bone marrow stromal stem cells express germline, ectodermal, endodermal, and mesodermal genes prior to neurogenesis. Journal of neuroscience research 69(6):908-917.

Figure Legends

Figure 1. Approach of GFP-labeled MSCs to neuronal axons in spinal roots.

GFP-labeled MSCs were injected into the subarachnoid space at the level of the lumber spinal cord. (A) A low magnification HE staining image of a spinal section immediately after the injection. (B) A magnified image of the region surrounded by a white square in (A). (C) An immunofluorescence image of the same region in (B) for MBP (red) and GFP (green). Dotted lines indicate the dura and arachnoid mater. (D-G) Spinal sections that were double immunostained for MBP (red) and GFP (green) at 1 hour (D, E) or 3 days (F, G) after the injection. The regions surrounded by white squares in (D) and (F) are magnified in (E) and (G), respectively. Scale bars, 100 μm in (A), (B), (C), (D), (F) and 20 μm in (E), (G).

Figure 2. Axonal degeneration precedes myelin degeneration in spinal motor neurons of SCA1-KI mice.

Double immunofluorescence staining of the ventral root of the lumber spinal cord from the WT (A, D, G) and SCA1-KI (B, E, H) mice at 7 months of age (7M) (A, B), 3 months of age (3M) (D, E) and 1 month of age (1M) (G, H) with anti-β-tubulin and anti-MBP antibodies. The diameters of β-tubulin-labeled axons and inner diameters of MBP-stained myelin sheaths were quantified and compared between the WT and SCA1-KI mice at ages of 7 months (n = 40 and 60 in 4 and 6 sections from 2 WT and 3 KI mice, respectively) (C), 3 months (n = 60 and 40 in 6 and 4 sections from 3 WT and 2 KI mice, respectively) (F) and 1 month (n = 120 and 120 in 12 and 12 sections from 3 WT and 3 KI mice, respectively) (I). Scale bar, 10 μm. ***$p < 0.001$.

Figure 3. MSCs attenuate the degeneration of both axons and myelin of spinal motor neurons in SCA1-KI mice.

(A) The ventral root of the lumber spinal cord from 7-month-old WT, untreated SCA1-KI (naive) and MSC-treated SCA1-KI (MSCs) mice. The images were double immunolabeled for β-tubulin (left, green) and MBP (middle, red) and then merged (right). (B, C) The diameters of axons (B) and myelin sheaths (C) were quantified in the WT (n = 40 axon and myelin pairs in 4 sections from 2 mice), untreated SCA1-KI (naive) (n = 60 axon and myelin pairs in 6 sections from 3 mice) and MSC-treated SCA1-KI (MSCs) (n = 60 axon and myelin pairs in 6 sections from 3 mice) mice. Scale bar, 20 μm. ***$p < 0.001$.

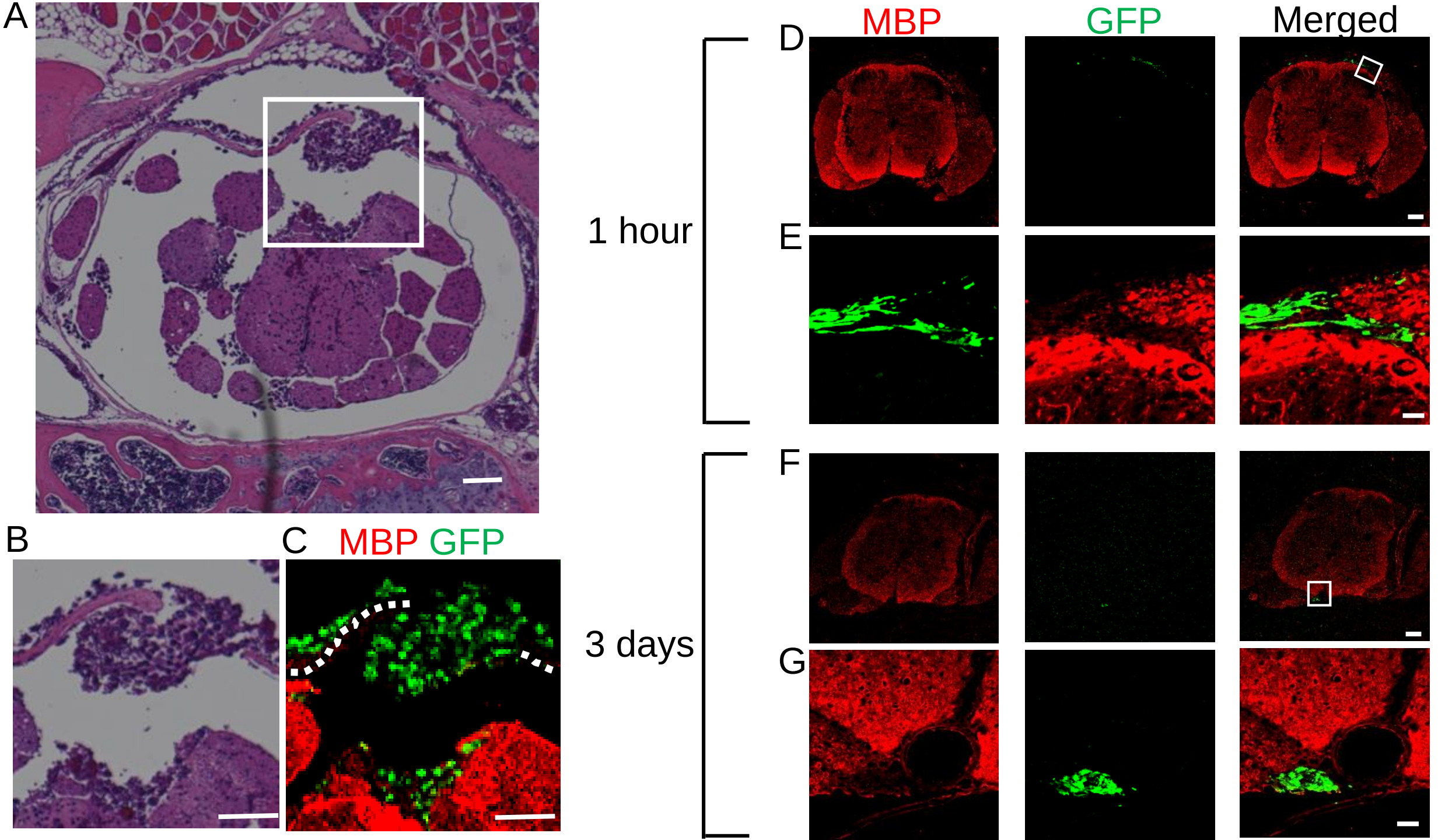
A
B
C
MBP GFP
1 hour
3 days
D
E
F
G
MBP
GFP
Merged

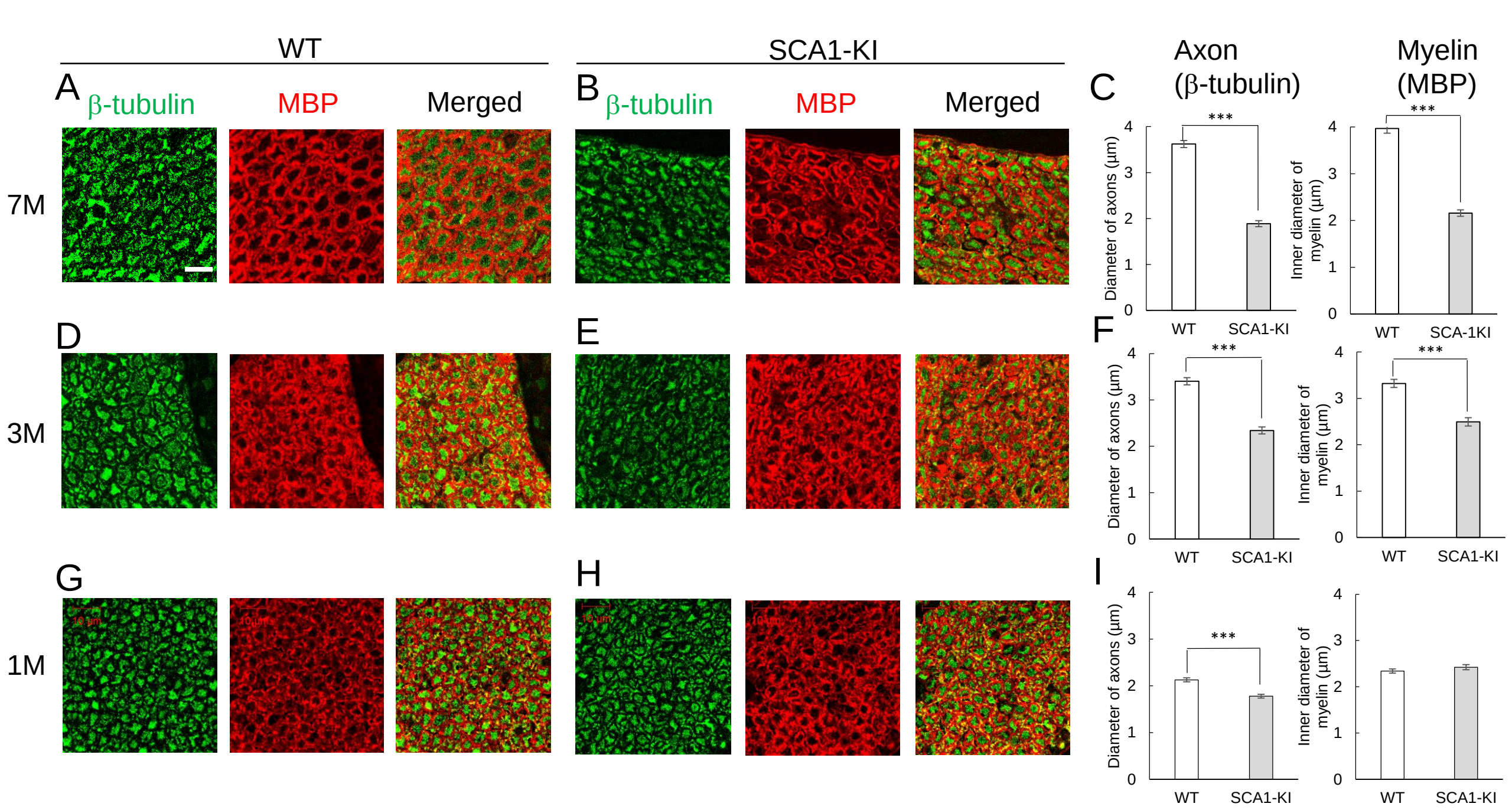
WT
SCA1-KI
A
β-tubulin
MBP
Merged
B
β-tubulin
MBP
Merged
7M
C
Axon (β-tubulin)
Myelin (MBP)
Diameter of axons (μm)
Inner diameter of myelin (μm)
***
WT
SCA1-KI
SCA-1KI
D
E
3M
F
G
H
1M
I
10 μm

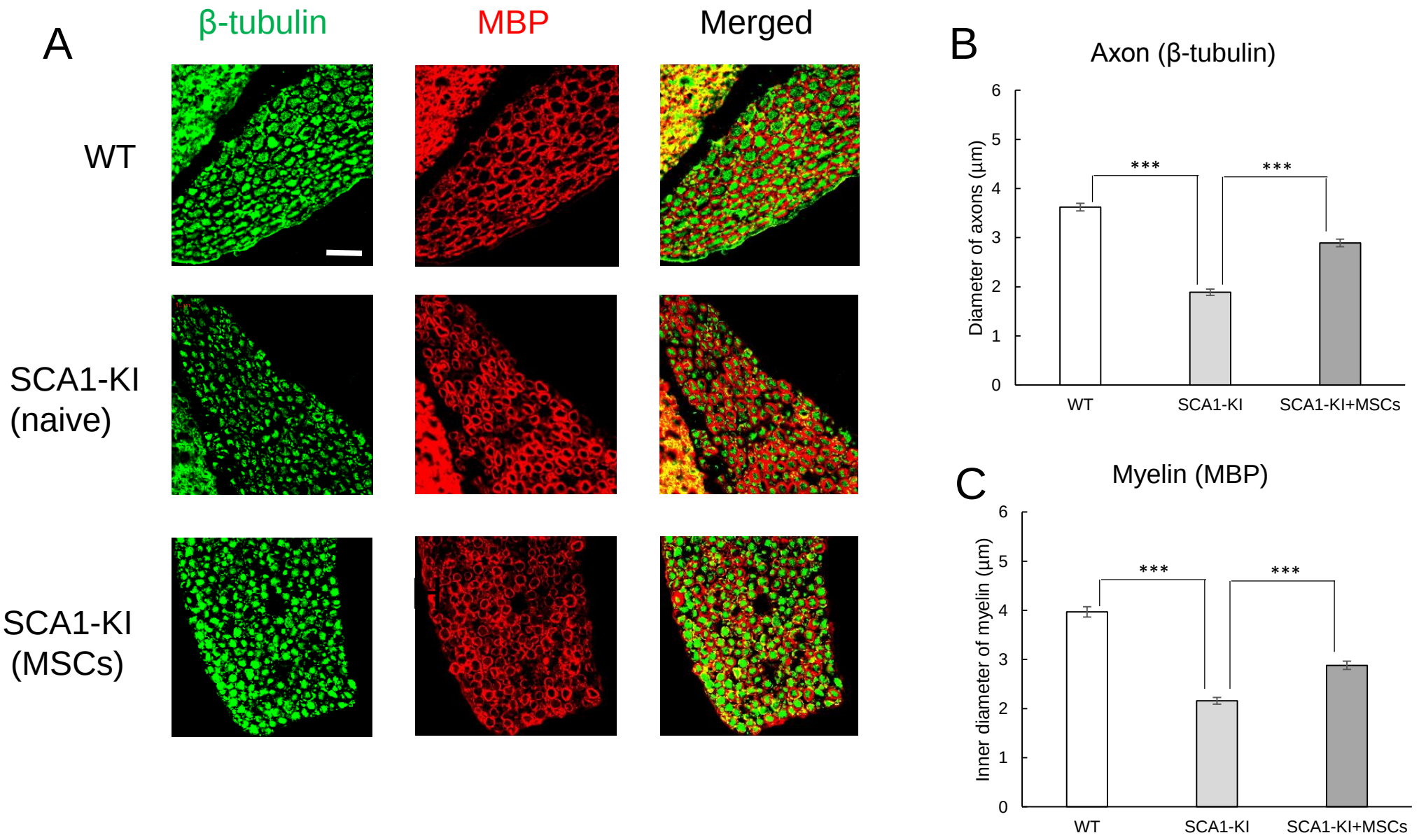
A
β-tubulin
MBP
Merged
WT
SCA1-KI
(naive)
SCA1-KI
(MSCs)
B
Axon (β-tubulin)
Diameter of axons (μm)
0
1
2
3
4
5
6
***
***
WT
SCA1-KI
SCA1-KI+MSCs
C
Myelin (MBP)
Inner diameter of myelin (μm)
0
1
2
3
4
5
6
***
***
WT
SCA1-KI
SCA1-KI+MSCs